



## Removal of oxidized sulfur compounds using different types of activated carbon, aluminum oxide, and chitosan-coated bentonite

Ming-Chun Lu<sup>a</sup>, Michelle L. Agripa<sup>b</sup>, Meng-Wei Wan<sup>c,\*</sup>, Maria Lourdes P. Dalida<sup>b</sup>

<sup>a</sup>Department of Environmental Resources Management, Chia Nan University of Pharmacy and Science, Tainan, Taiwan

<sup>b</sup>Department of Chemical Engineering, University of the Philippines, Quezon City, Philippines

<sup>c</sup>Department of Environmental Engineering and Science, Chia Nan University of Pharmacy and Science, Tainan, Taiwan

Email: peterwan@mail.cna.edu.tw

Received 7 April 2013; Accepted 15 April 2013

### ABSTRACT

The adsorption of benzothiophene sulfone and dibenzothiophene sulfone from diesel using six different types of adsorbents were investigated. Adsorbents used were commercial adsorbents granular-activated carbon (GAC), aluminum oxide (ALU), novel adsorbents chitosan-coated bentonite (CHB), and metal-ion impregnated activated carbons, where there types of metal ions,  $\text{Cu}^{2+}$ ,  $\text{Fe}^{3+}$ , and  $\text{Ni}^{2+}$ , were loaded ( $\text{Cu}^{2+}/\text{AC}$ ,  $\text{Fe}^{3+}/\text{AC}$ ,  $\text{Ni}^{2+}/\text{AC}$ ). Kinetic studies conducted showed that the adsorption process followed a pseudo-second-order kinetics. Equilibrium studies indicated that the heterogeneous and homogenous monolayer adsorption and are present in the process. Moreover, based on the results of sulfone removal using the synthetic diesel fuel, increasing removal efficiencies of Benzothiophene sulfone followed the order of  $\text{ALU} < \text{GAC} < \text{Cu}^{2+}/\text{AC} < \text{Fe}^{3+}/\text{AC} < \text{CHB}$ , while for dibenzothiophene sulfone (DBTO) removal, increasing DBTO removed efficiencies followed the order of  $\text{GAC} < \text{CHB} < \text{ALU} < \text{Cu}^{2+}/\text{AC} \approx \text{Fe}^{3+}/\text{AC} \approx \text{Ni}^{2+}/\text{AC}$ .

**Keywords:** Desulfurization; Adsorption; Sulfone; Activated carbon; Aluminum oxide; Chitosan-coated bentonite (CHB)

### 1. Introduction

The petroleum industry faces a big challenge with regards to the production of clean fuel. The US Environmental Protection Agency (US EPA) has set the limits of sulfur content to 15 mg/kg for diesel and 30 mg/kg for gasoline fuels [1]. The conventional method of removing sulfur from hydrocarbon fuels is

through hydrodesulfurization, where the sulfur is converted to hydrogen sulfide at high temperature and pressure in the presence of noble catalysts. But this method entails high operating cost. Also, HDS is limited, when it comes to removing benzothiophenes (BTs) and dibenzothiophene (DBTs) [2].

Alternative methods of removing sulfur from diesel fuel have already been under study desulfurization (ADS) utilizes an active adsorbent, which is a porous,

\*Corresponding author.

Presented at the Fifth Annual International Conference on “Challenges in Environmental Science & Engineering—CESE 2012” Melbourne, Australia, 9–13 September 2012

nonreactive substrate that allows high surface area for the adsorption of sulfur compounds [2,3]. Biodesulfurization utilizes microorganisms in removing sulfur compounds from fuels. Advantages presented by this alternative process are as follows: (a) it is carried out in mild temperature and pressure conditions which makes it an energy-saving process, and (b) since it is a biological activity, biocatalysts involved would be highly selective [4]. Moreover, oxidative desulfurization (ODS) principle depends on sulfur compounds having more affinity to oxidation than their analogue hydrocarbons in fossil fuels [5]. Since the oxidized compounds are still present in the fuel after undergoing the oxidation process, another step is needed to remove it. Therefore, the ODS is usually accompanied by extraction or adsorption of the sulfones.

Based on previous studies, many adsorbents have been invented and applied to different purposes of contaminations removal. Commercial adsorbents activated carbon and aluminum oxide (ALU) have been known as effective adsorbent for many applications [6]. Chitosan-coated bentonite (CHB) has been tested in removing heavy metals from aqueous solutions [7,8]. Metal ion-impregnated activated carbons have been used in removing BT and DBT [9].

This study aims to remove oxidized sulfur compounds, particularly benzothiophene sulfone (BTO) and dibenzothiophene sulfone (DBTO) from model diesel fuel using different adsorbents, namely commercial adsorbents granular-activated carbon (GAC) and ALU, and novel adsorbents CHB and ion-impregnated activated carbons.

## 2. Materials and methods

### 2.1. Chemicals and commercial adsorbents

The chemicals used in the study were reagent grade. BTO and DBTO were obtained from Sigma–Aldrich. Toluene was from Merck. Cupric nitrate 2.5 hydrate,  $(\text{Cu}(\text{NO}_3)_2 \cdot 2.5(\text{H}_2\text{O}))$ , was purchased from JT Baker, while ferric nitrate nonahydrate,  $(\text{Fe}(\text{NO}_3)_3 \cdot 9(\text{H}_2\text{O}))$ , and nickel (II) nitrate hexahydrate  $(\text{Ni}(\text{NO}_3)_2 \cdot 6(\text{H}_2\text{O}))$  and were analytical reagents from Merck. Low-molecular-weight chitosan powder was obtained from Aldrich of Sigma–Aldrich, USA. Bentonite, with assay  $\text{SiO}_2$ : 61.32%,  $\text{Al}_2\text{O}_3$ : 19.78% was procured from first chemical reagents. Moreover, adsorbents GAC and ALU were purchased from E. Comis, Taiwan.

### 2.2. Preparation and characteristic analysis of CHB

Procedure was based on the study of Futralan and colleagues [7,8]. Chitosan was dissolved in 5% v/v

HCl and stirred for 2 h at 300 rpm. About 100 g of bentonite was added to the solution and stirred for another 3 h. Dropwise addition of 1 N NaOH was done until neutralization occurs. The adsorbent was washed and dried at 65°C for 24 h. The dried adsorbent was sieved, and the particle size 0.21–0.5 mm was used in the batch studies.

Thermal gravimetric analyses (TGA) were performed on freeze-dried bentonite, chitosan, and CHB samples using Rigaku Thermo Plus TG 8120 in the temperature range of 30–800°C at a heating rate of 10°C per min.

### 2.3. Preparation of ion-impregnated activated carbons

Procedure was based on study of Xiao and colleagues [9]. About 10 g of activated carbon were added to 100 mL of 0.1 M metal nitrate ( $\text{Cu}(\text{NO}_3)_2$ ,  $\text{Fe}(\text{NO}_3)_3$ , and  $\text{Ni}(\text{NO}_3)_2$ ) at room temperature. The samples were filtered after 12 h and dried 393 K for 5 h.

### 2.4. Adsorption equilibrium studies

Solutions of BTO and DBTO were prepared with a concentration of 500 mg/L by dissolving BTO and DBTO in benzene. Different adsorbents illustrated in Table 1 were examined by batch adsorption study. Approximately, 1 g of the adsorbents and 10 mL were placed in stoppered Erlenmeyer flasks. The solution was agitated at 120 rpm for contact times ranging from 5 min to 24 h. The solutions were maintained at a temperature of 25°C. The adsorption capacity was calculated as Eq. (1):

$$q_e = \frac{(C_0 - C_e)W}{W} \quad (1)$$

where  $C_0$  is the initial concentration (mg/L),  $C_e$  is the equilibrium concentration (mg/L), and  $W$  is the weight of the adsorbent (g).

The percentage removal of adsorbate is computed as follows:

Table 1

The deferent adsorbents used in this study and their abbreviation

Adsorbents	Abbreviation
Granular-activated carbon	GAC
Aluminum oxide	ALU
Chitosan-coated bentonite	CHB
Copper ion-impregnated activated carbons	$\text{Cu}^{2+}/\text{AC}$
Ferric ion-impregnated activated carbons	$\text{Fe}^{3+}/\text{AC}$
Nickel ion-impregnated activated carbons	$\text{Ni}^{2+}/\text{AC}$

$$\% \text{ Removal} = \left( \frac{C_0 - C_e}{C_0} \right) \times 100 \quad (2)$$

where  $C_0$  and  $C_e$  are the initial and equilibrium concentrations, respectively.

### 2.5. Adsorption kinetic studies

Kinetic studies were conducted to determine the rate of the adsorption process. Kinetic equations of the pseudo-first-order and pseudo-second-order were used. The pseudo-first-order rate equation is Eq. (3):

$$\ln(q_e - q) = \ln q_e - k_1 t \quad (3)$$

where  $q$  is the amount adsorbed at time  $t$ ,  $q_e$  is the equilibrium amount, and  $k_1$  is the pseudo-first-order kinetic constant. The pseudo-second-order rate equation has the form as Eq. (4):

$$\frac{t}{q} = \frac{1}{k_2 q_e^2} + \frac{1}{q_e} t \quad (4)$$

where  $k_2$  is the pseudo-second-order kinetic constant.

### 2.6. Adsorption isotherm studies

BTO and DBTO solutions with concentrations ranging from 100 mg/L to 1,000 mg/L were used. In stoppered Erlenmeyer flasks, 1.0 g of the adsorbents and 20 mL of the solutions were added and stirred at 120 rpm for 48 h maintained at 25 °C.

The Langmuir and Freundlich isotherm models were used to describe the adsorption equilibrium. From these models, adsorption performance of the adsorbents could be evaluated. The adsorption capacity of the adsorbent was calculated, and equation constants that give indications of adsorption performance were also determined.

### 2.7. Preparation of the synthetic diesel fuel

BTO and DBTO were weighed and dissolved in commercial diesel to make a 500 mg/L BTO, and 500 mg/L DBTO mixed solution, which were used to examine the sulfone removal efficiencies by using different adsorbents.

### 2.8. Analytical methods and instrumentation

To determine the amount of oxidized sulfur in the solution, the Agilent Technologies 7890A gas chromatography (GC) system equipped with a fused-silica capillary HP-5 ms column (30 m) having a thickness of 0.25-mm film (J & W Scientific, Folsom, CA USA)

was employed. The GC was connected to a sulfur chemiluminescence detector for higher selectivity and sensitivity toward ultra low sulfur concentration. The GC temperature was initially set to 100 °C for 3 min and ramped to 300 °C at increasing rate of 20 °C/min.

## 3. Results and discussion

### 3.1. Characteristic analysis of adsorbent

To confirm the successful immobilization of chitosan onto bentonite, the results from TGA analysis are presented in Fig. 1. The chitosan has two decomposition sites: the first one is at 240 °C and the second is at 320 °C. It was then completely burnt out at 600 °C. The carriers, bentonite, has two sites that indicate the weight loss at 90 °C and 600 °C. The thermogram of CHB that shows similar decomposition stages of chitosan with a relatively less weight loss indicates that about 5.5% of chitosan is successfully coated on bentonite.

### 3.2. Kinetic studies

Kinetic studies give an indication on how fast the adsorption process occurs, and how long until equilibrium is reached. Fig. 2 shows the ratio of the remaining sulfur to its initial concentration as contact time progressed. The graph implies that the rate of adsorption consists of two steps, a very fast rate during the first five minutes and a slow rate until equilibrium is reached.

Table 2 shows the calculated kinetic constants and the correlation coefficients ( $R^2$ ) for the pseudo-first- and pseudo-second-order fit for the adsorption of BTO and DBTO. The  $R^2$  values for the pseudo-second-order gave higher values, which indicate that the

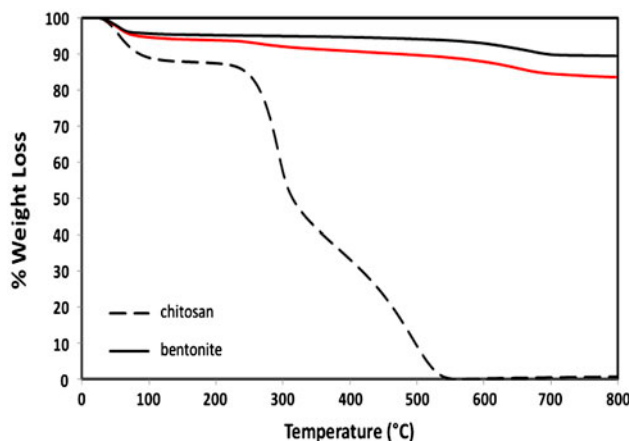


Fig. 1. TGA of CHB.

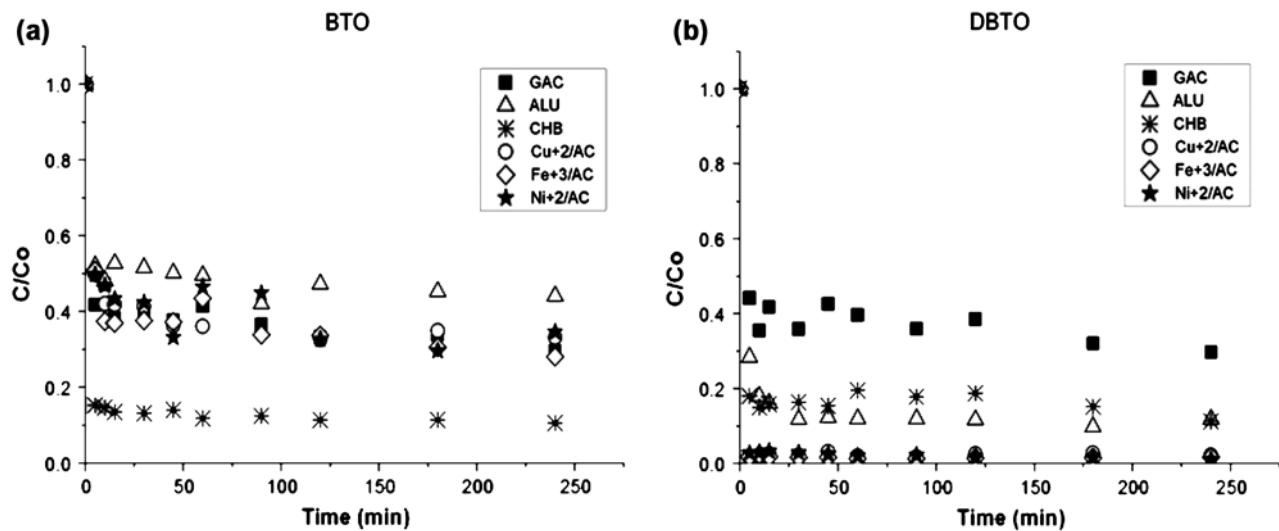


Fig. 2.  $C/C_0$  vs. contact time using all adsorbents,  $C_0=500$  mg/L,  $m=1.0$  g adsorbent,  $25^\circ\text{C}$ . (a) for BTO removal; (b) for DBTO for removal.

adsorption processes follow this pseudo-second-order order. This implies that chemisorption is the predominant mechanism in the adsorption of BTO and DBTO onto the selected adsorbents.

The overall adsorption rate for both ions appeared to be controlled by the chemical process. The conclusion is based on the assumption that chemisorption involved valence forces, via sharing or exchange of electrons as covalent forces between the transition metal cations and adsorbent and ion exchange [10]. Moreover, comparing the values of  $q_{e,\text{exptl}}$  and  $q_{e,\text{cal}}$  in the pseudo-second-order constants, the values are

within 1% of each other, which further supports the finding that the adsorption follows the pseudo-second-order rate.

### 3.3. Adsorption isotherms

The adsorption data were evaluated using the Langmuir and the Freundlich isotherm models, which are the most common models used for examining adsorption data. The calculated correlation coefficients gave high values for both the Langmuir and Freundlich isotherm models. Fig. 3 shows the equilibrium

Table 2  
Kinetic parameters for the pseudo-first-order and pseudo-second-order models

Sulfur compound	Adsorbent	$q_{e,\text{exptl}}$	Pseudo-first-order model constants			Pseudo-second-order constants		
			$k_1$	$q_{e,\text{cal}}$	$R^2$	$k_2$	$q_{e,\text{cal}}$	$R^2$
BTO	GAC	3.5200	0.0072	0.6549	0.6637	0.0552	3.4928	0.9966
	ALU	2.7940	0.00953	0.41321	0.7643	0.11177	2.80269	0.9980
	CHB	4.9255	0.02131	0.07502	0.3017	2.07707	4.92611	0.99997
	$\text{Cu}^{2+}/\text{AC}$	3.3360	0.0098	0.4937	0.4713	0.0899	3.3445	0.9971
	$\text{Fe}^{3+}/\text{AC}$	3.5930	0.0089	0.7283	0.6629	0.0475	3.5945	0.9957
	$\text{Ni}^{2+}/\text{AC}$	3.5180	0.0056	0.7253	0.2340	0.0538	3.3921	0.9885
DBTO	GAC	3.5027	0.0069	0.6807	0.4167	0.0533	3.4819	0.9950
	ALU	4.5047	0.01570	0.39388	0.5001	1.05112	4.43262	0.9998
	CHB	4.4360	-0.00021	0.26794	0.1409	0.09342	4.36110	0.9976
	$\text{Cu}^{2+}/\text{AC}$	4.9000	0.0010	0.0275	0.1734	11.9954	4.8804	0.99997
	$\text{Fe}^{3+}/\text{AC}$	4.9276	0.0090	0.0232	0.1867	4.9939	4.9237	0.999996
	$\text{Ni}^{2+}/\text{AC}$	4.9358	0.0096	0.0985	0.8451	0.4675	4.9358	0.99998

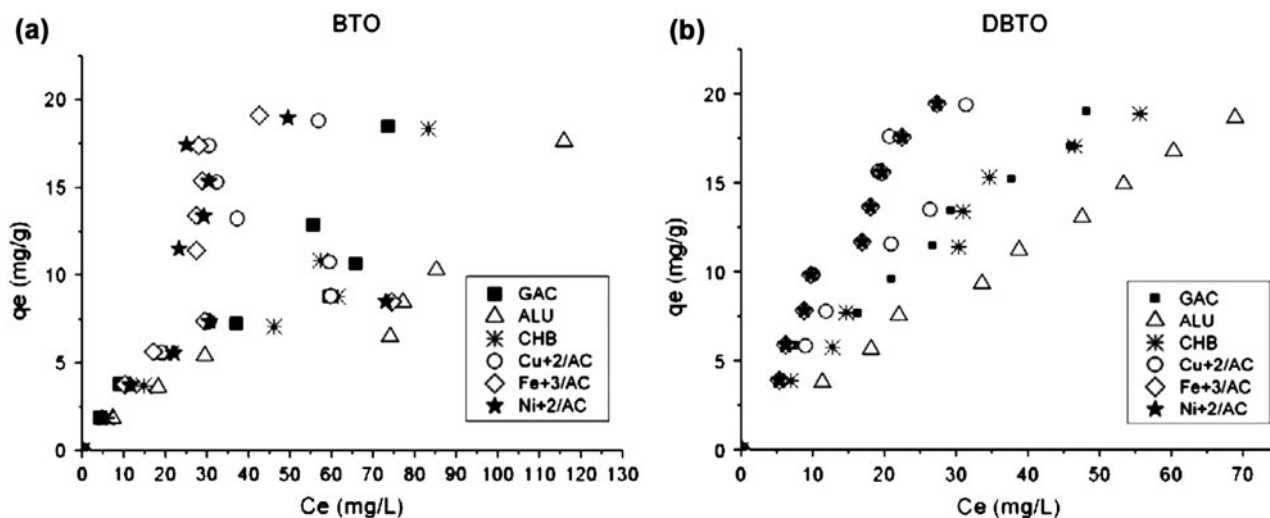


Fig. 3. Equilibrium adsorption isotherms on all adsorbents.  $C_0 = 100\text{--}1,000\text{ mg/L}$ ,  $m = 1.0\text{ g}$  adsorbent,  $T = 25^\circ\text{C}$ . (a) BTO removal; (b) DBTO removal.

Table 3  
Adsorption isotherm constants for all adsorbents

Sulfur compound	Adsorbent	Langmuir model			Freundlich model		
		$b$	$q_{\max}$	$R^2$	$k_f$	$n$	$R^2$
BTO	GAC	0.0340	15.72	0.9803	0.7967	1.547	0.9088
	ALU	0.1927	14.79	0.9728	0.4643	1.438	0.9047
	CHB	0.0154	18.55	0.9796	0.4819	1.317	0.9293
	$\text{Cu}^{2+}/\text{AC}$	0.00987	39.84	0.7458	0.9603	1.494	0.4137
	$\text{Fe}^{3+}/\text{AC}$	0.00652	63.69	0.6586	1.5153	1.758	0.2233
	$\text{Ni}^{2+}/\text{AC}$	0.00816	50.10	0.9037	4.0513	1.282	0.5435
DBTO	GAC	0.0382	24.15	0.9661	1.3630	1.511	0.9757
	ALU	0.0052	68.03	0.9935	0.4614	1.147	0.9922
	CHB	0.0015	40.49	0.9830	0.8614	1.279	0.9778
	$\text{Cu}^{2+}/\text{AC}$	0.01180	69.93	0.7414	1.2465	1.265	0.7229
	$\text{Fe}^{3+}/\text{AC}$	0.02111	51.28	0.9656	1.078	1.128	0.9491
	$\text{Ni}^{2+}/\text{AC}$	0.02748	35.17	0.9002	0.501	0.9724	0.8021

adsorption isotherms for the removal of BTO and DBTO using all the adsorbents.

The Langmuir model has the linearized form, shown as Eq. (5) [11]:

$$\frac{1}{q_e} = \frac{b}{q_{\max}} + \frac{1}{q_{\max}C_e} \quad (5)$$

where  $q_e$  is the amount adsorbed at equilibrium (mg/g),  $C_e$  is the amount of the adsorbate in solution at equilibrium (mg/L),  $q_{\max}$  is the maximum monolayer capacity of the adsorbent (mg/g), and  $b$  is the

affinity of the adsorbates to the binding site (L/mg). By making a linear plot of  $1/q_e$  vs.  $1/C_e$ , the corresponding constants can be determined.

The Freundlich isotherm has the linear form, as shown in Eq. (6):

$$\log q_e = \log k_f + \frac{1}{n} \log C_e \quad (6)$$

where  $q_e$  (mg/g) is the amount of sulfur compound adsorbed at equilibrium,  $C_e$  (mg/L) is the remaining concentration of the solution at equilibrium,  $k_f$  is an indicator of the adsorption capacity, while  $n$  is related

Table 4  
Comparison of BTO and DBTO adsorption capacities of different adsorbents used

Sulfur compound	Adsorbent	Adsorption capacity (mg/g)	Surface area (m <sup>2</sup> )	Adsorption capacity (mg/m <sup>2</sup> )
BTO	GAC	15.72	1,100	0.0143
	ALU	14.79	322	0.0459
	CHB	18.55	33.17	0.5590
	Cu <sup>2+</sup> /AC	39.84	1,110	0.0359
	Fe <sup>3+</sup> /AC	63.69	1,077	0.0591
	Ni <sup>2+</sup> /AC	50.10	1,145	0.0438
DBTO	GAC	24.15	1,100	0.0220
	ALU	68.03	322	0.2110
	CHB	40.49	33.17	1.2200
	Cu <sup>2+</sup> /AC	69.93	1,110	0.0630
	Fe <sup>3+</sup> /AC	51.28	1,077	0.0476
	Ni <sup>2+</sup> /AC	35.17	1,145	0.0307

to the magnitude of the adsorption driving force and to the distribution of the energy sites on the adsorbent [12]. Plotting  $\log q_e$  vs.  $\log C_e$  would enable the calculation of the isotherm constants.

Table 3 shows the calculated isotherm constants using the two isotherm models. The Langmuir model gave higher correlation coefficient ( $R^2$ ) values which imply that the adsorption process can be better described by the Langmuir model. This indicates that there is homogeneous monolayer adsorption on the surface of the adsorbents. But it is noted that the  $R^2$  values for the Freundlich model are also relatively high, and therefore cannot just be disregarded. There is, therefore, an indication that homogeneous adsorption is not the only mechanism involved. The presence of heterogeneous adsorption is therefore implied, which supports the initial finding that the kinetics follows the pseudo-second-order rate.

In Table 3, the calculated values of  $n$  for all adsorbents except Ni<sup>2+</sup>/AC gave values greater than one ( $n > 1$ ), which indicates favorable condition and good adsorption of BTO and DBTO onto the adsorbents.

Table 5  
Comparison of % BTO and DBTO removal using different adsorbents

Sulfur compound	% Removal					
	GAC	ALU	CHB	Metal ion-impregnated GAC		
				Cu <sup>2+</sup> /AC	Fe <sup>3+</sup> /AC	Ni <sup>2+</sup> /AC
BTO	70.47	55.92	98.56	66.88	71.92	65.35
DBTO	70.34	88.19	88.75	97.81	98.34	98.96

Table 4 gives the values of adsorption capacity of each adsorbent for BTO and DBTO removal. In removing BTO, the adsorption capacity (mg/m<sup>2</sup>) followed the order of ALU (14.79) < GAC (15.72) < CHB (18.55) < Cu<sup>2+</sup>/AC (39.84) < Ni<sup>2+</sup>/AC (50.10) < Fe<sup>3+</sup>/AC (63.69). Fe<sup>3+</sup>/AC illustrates the highest capacity, while ALU has the least. Moreover, in removing DBTO, the adsorption capacity (mg/m<sup>2</sup>) followed the order of GAC (24.15) < Ni<sup>2+</sup>/AC (35.17) < CHB (40.49) < Fe<sup>3+</sup>/AC (51.28) < ALU (68.03) < Cu<sup>2+</sup>/AC (69.93). Cu<sup>2+</sup>/AC has the highest capacity, and unmodified GAC adsorbed the least.

Adsorption capacity can also be expressed in terms of capacity per area. From Table 4, CHB has the highest capacity per unit area for both BTO and DBTO. This is due to the small surface area of the CHB, even if it did not adsorb the largest amount of adsorbate present. Moreover, it is essential to indicate that the adsorption capacities of the ion-impregnated activated carbon are all higher than the adsorption capacity of the unmodified GAC, which supports the result that impregnating activated carbon with metal ions increases its BTO and DBTO uptake or removal.

#### 3.4. Sulfone removal using the synthetic diesel fuel

Table 5 summarizes the adsorption efficiency of GAC, ALU, CHB and the metal ion-impregnated GAC in removing BTO and DBTO from synthetic diesel fuel. The result indicates that the modified activated carbon adsorbed DBTO better, up to 98% removal. The adsorption efficiency though three adsorbents illustrates almost the same performance. Moreover, for BTO removal, the CHB illustrates the highest removal performance.

#### 4. Conclusions

The adsorption rate of BTO and DBTO onto the adsorbents used occurred initially at a very fast rate, then at a slower pace until equilibrium was reached.

Kinetic studies on the removal of the oxidized sulfur compounds showed that the adsorption followed the pseudo-second-order rate model. Equilibrium studies indicate that the adsorption process gave high correlations for both Langmuir and Freundlich isotherm models, which suggest the presence of physisorption and chemisorption.

Among the adsorbents, the CHB gave the highest removal of BTO from diesel, while the ion-impregnated activated carbons had better DBTO removal than the other adsorbents though the three had almost the same performance.

### Acknowledgment

The authors would like to thank the National Science Council of Taiwan, for financially supporting this research under Contract No. NSC 99-2221-E-041-012-MY3 and NSC 101-2221-E-041-010-MY3.

### References

- [1] US EPA Regulatory Announcement: Heavy-Duty Engine and Vehicle Standards and Highway Diesel Fuel Sulfur Control Requirements, December 2000.
- [2] A. Srivastav, V.C. Srivastava, Adsorptive desulfurization by activated alumina, *J. Hazard. Mater.* 170 (2009) 1133–1140.
- [3] M. Muzic, K.S. Bionda, Z. Gomzi, S. Podolski, S. Telen, Study of diesel fuel desulfurization by adsorption, *Chem. Eng. Res. Des.* 88 (2010) 487–495.
- [4] M. Soleimani, A. Bassi, A. Margaritis, Biodesulfurization of refractory organic sulfur compounds in fossil fuels, *Biotechnol. Adv.* 25 (2007) 570–596.
- [5] O. Etemadi, T.F. Yen, Aspects of selective adsorption among oxidized sulfur compounds in fossil fuels, *Energy Fuels* 21 (2007) 1622–1627.
- [6] Y.S. Ho, G. McKay, A comparison of chemisorption kinetic models applied to pollutant removal on various sorbents, *Trans. IChemE* 76 (1998) 332–340.
- [7] C.M. Futralan, C.C. Kan, M.L. Dalida, K.J. Hsien, C. Pascua, M.W. Wan, Comparative and competitive adsorption of copper, lead, and nickel using chitosan immobilized on bentonite, *Carbohydr. Polym.* 83 (2011) 528–536.
- [8] C.M. Futralan, C.C. Kan, M.P. Dalida, C. Pascua, M.W. Wan, Fixed-bed column studies on the removal of copper using chitosan immobilized on bentonite, *Carbohydr. Polym.* 83 (2011) 697–704.
- [9] J. Xiao, Z. Li, B. Liu, O. Xia, O. Yu, Adsorption of benzothiophene and dibenzothiophene on ion-impregnated activated carbons and ion-exchanged  $\gamma$ -zeolites, *Energy Fuels* 22 (2008) 3858–3863.
- [10] M.W. Wan, C.C. Kan, B.D. Rogel, M.L. Dalida, Adsorption of copper (II) and lead (II) ions from aqueous solution on chitosan-coated sand, *Carbohydr. Polym.* 80 (2010) 891–899.
- [11] I. Langmuir, The adsorption of gases on plane surfaces of gas, mica, and platinum, *J. Am. Chem. Soc.* 40 (1918) 1361–1403.
- [12] T. Karanfil, J.E. Kilduff, Role of granular activated carbon surface chemistry on the adsorption of organic compounds. 1. Priority pollutants, *Environ. Sci. Technol.* 33 (1999) 3217–3224.